Data report: particle size analysis of Nankai Trough sediments, IODP Expedition 338 Site C0021[1]

Zachary T. Moore[2] and Derek E. Sawyer[3]

Chapter contents

Abstract 1
Introduction 1
Methods 2
Samples 2
Results 3
Acknowledgments 3
References 3
Figures 4
Tables 12

[1] Moore, Z.T., and Sawyer, D.E., 2014. Data report: particle size analysis of Nankai Trough sediments, IODP Expedition 338, Site C0021. *In* Strasser, M., Dugan, B., Kanagawa, K., Moore, G.F., Toczko, S., Maeda, L., and the Expedition 338 Scientists, *Proc. IODP,* 338: Yokohama (Integrated Ocean Drilling Program). doi:10.2204/iodp.proc.338.201.2014
[2] Earth and Environmental Sciences, University of Kentucky, Lexington KY 40511, USA. zachary.moore@uky.edu
[3] School of Earth Sciences, The Ohio State University, Columbus OH 43210, USA.

Abstract

Hydrometer analysis of 49 sediment samples from Integrated Ocean Drilling Program (IODP) Expedition 338 Site C0021, offshore Japan, indicates two lithologies: clayey silt (80% of samples) and silty clay (20% of samples). Samples were collected at approximately 1 sample per 2 m from 0.06 and 83.6–193.7 meters below seafloor. Samples were selected with the primary objective of determining particle size distribution within two mass transport deposits (MTD-A and MTD-B) and to establish the background "non-MTD" particle size distribution. We performed hydrometer analyses because of the fine-grained nature of the sediments. Clayey silt is composed primarily of silt-size particles (>50 wt%) with 25–50 wt% clay-sized particles and <20 wt% sand-sized particles. Silty clay is composed primarily of clay-sized particles (50 wt%) with 25–50 wt% silt-sized particles and <20 wt% sand-sized particles. Samples from MTD-A plot within the silty clay and clayey silt fields, whereas samples from MTD-B plot exclusively in the clayey silt field.

Introduction

The Nankai Trough Seismogenic Zone Experiment (NanTroSEIZE) is dedicated to studying the fault mechanics and seismogenesis of the thrusting Philippine Sea plate under the Eurasian plate by drilling, logging boreholes, 3-D seismic imaging, core sampling, and modeling (see the **"Expedition 338 summary"** chapter [Strasser et al., 2014]). During IODP Expedition 338, a slope basin seaward of the megasplay was logged and cored at Site C0021 (Figs. **F1, F2**). The slope basin, characterized in 3-D seismic data by stacked mass transport deposits (MTDs) (Strasser et al., 2011), was drilled and sampled in Hole C0018A during Expedition 333 and logged during Expedition 338 to define the Quaternary mass-movement event stratigraphy and to analyze physical properties to constrain sliding dynamics and tsunamigenic potential. During Expedition 338, logging while drilling (LWD) to 294 meters below seafloor (mbsf) and coring to 194.5 mbsf were conducted at Site C0021. This site is located ≈2 km northwest of Site C0018 and at a more proximal site for MTDs than observed at Site C0018 (Fig. **F2**). LWD and coring at Site C0021 therefore provide important information on the nature, provenance, and kinematics of MTDs.

doi:10.2204/iodp.proc.338.201.2014

Particle size distribution is a fundamental property that plays a key role in the dynamic behavior of submarine landslides (Sawyer et al., 2012). Our objective was to measure downcore particle size distributions with focus on the MTDs. We used hydrometer particle size analysis and classified sediment type according to the Shepard (1954) classification (Fig. F3). We analyzed 49 samples (Table T1) collected at the Kochi Coring Facility, Japan, in April 2013.

Methods

Particle size analysis was conducted at the University of Kentucky (USA) using the standard hydrometer method for mud-dominated samples (ASTM, 2007). Sawyer et al. (2008) present similar hydrometer analyzes on fine-grained sediments from within and without MTDs in the Ursa Basin.

Principles of hydrometer analysis

Hydrometer analysis is based on Stokes' law, which defines the terminal velocity of a spherical particle settling through a column of fluid. Stokes' law assumes all particles are spherical and settle at different rates based on the size of each particle. A hydrometer measures the density of the mixture at a known depth below the surface. The density of the suspension is based on the specific gravity and amount of sediment. The density of the mixture decreases as the particles settle out of the suspension. From the hydrometer readings, calculations provide the maximum particle diameter (D, in mm) at a specific time (Eq. 1) and the percentage of the original sample mass that is smaller than the particle diameter (mm) at the specific time, and thus, still in suspension (Eq. 2) (Germaine and Germaine, 2009). Variables are detailed in Table T2.

$$D = \sqrt{\frac{18\mu}{\rho_w g(G_s - 1)}} \times \sqrt{\frac{H}{t}} \quad (1)$$

where

H = distance particle falls (cm),
ρ_w = mass density of water (g/cm^3),
G_s = specific gravity (dimensionless),
μ = viscosity of fluid (mPa·s),
g = acceleration due to gravity (cm/s^2), and
D = Diameter of particle (mm).

$$N_m = [G_s/(G_s - 1)] \times (V/M_D) \times \rho_c(r_m - r_{w,m}) \times 100, \quad (2)$$

where

N_m = percent finer material at reading m (%),
V = volume of suspension (cm^3),
M_D = dry soil mass of hydrometer specimen (g),
ρ_c = mass density of water at the calibration temperature (g/cm^3),
r_m = hydrometer reading in suspension at time t and temperature T (dimensionless),
$r_{w,m}$ = hydrometer reading in water with dispersant at the same temperature as for r_m (dimensionless), and
m = reading number.

Samples

A total of 49 (20 cm^3 plug) samples were chosen from Hole C0021B from 0 to 0.06 mbsf and from 83.6 to 194 mbsf. Coring was not conducted between 0.06 and 83.6 mbsf. Twenty-nine samples were collected from MTDs: 11 from MTD-A and 18 from MTD-B. The remaining 20 samples were selected to establish the background non-MTD particle size distribution. Moisture and density data for Site C0021 reveals a range of grain densities between 2.55 and 2.77 g/cm^3 and an average of 2.73 g/cm^3 for all 49 samples. Therefore, a density value of 2.7 was used in Eqs. 1 and 2, and the error associated with using this value is <5%.

Sample preparation

Sample preparation followed the ASTM hydrometer method (ASTM, 2007). We briefly summarize the method as follows:

1. Each sample was removed from its sealed plastic shipping bag, weighed, and placed into a 250 mL beaker.
2. Each sample was soaked for 12 h in 125 mL of 5% solution of deflocculant (sodium hexmetaphosphate [$Na_6P_6O_{18}$]).
3. Each sample was disaggregated by a malt mixer for 2 min and then wet-sieved through a 63 µm screen to separate sand-size particles.
4. The retained sand was dried and weighed for final percent sand calculations.
5. The remaining <63 µm slurry was transferred to a 1000 mL graduated cylinder and filled with deionized water to 1000 mL.
6. One control cylinder was prepared with 5% solution of dispersing agent and deionized water filled to 1000 mL. We measured the hydrometer reading and monitored the temperature. The laboratory temperature control system maintained a stable temperature environment, and thus there was little variation in viscosity. However, if the temperature fluctuated by 1°C, the resulting change in diameter was approximately 1%.

Hydrometer analysis

Before starting each experiment, samples were mixed for 2 min in the graduated cylinder using a plunger. The timer was started when the plunger was removed and the hydrometer was inserted. Hydrometer readings were taken at 15, 30, and 60 s without the hydrometer being removed. After the 60 s reading, the hydrometer was removed and rinsed in deionized water. The hydrometer was then reinserted, and readings were taken at 2, 4, 8, 16, 32 min, and so on until samples crossed the silt/clay boundary (2 µm), which typically occurred after a total settling time of 10–12 h. We recorded hydrometer readings to the nearest 0.1 g/L. An example hydrometer worksheet and graph are shown in Figures **F4** and **F5.** After each sample crossed the silt/clay boundary, it was dried and weighed for a final <62.5 µm dry mass.

Results

We present weight percent sand, silt, and clay for all samples in Table **T1.** Complete data sheets and particle size distribution curves similar to Figures **F4** and **F5** are included in Microsoft Excel format in HYDROMETER in **"Supplementary material."**

We plot particle size distributions on a ternary diagram according to the classification of Shepard (1954) (Figs. **F6, F7**) and as a downcore profile of weight percent sand, silt, and clay against LWD gamma ray and resistivity (Fig. **F8**).

The ternary classification defines two major lithologies (silty clay and clayey silt) and four minor lithologies (silt, sandy clay, sandy silt, and sand silt clay) (Fig. **F7**). Of the samples, 76% (37 of 49) are clayey silt, 16% (8) are silty clay, and 8% (4) are minor lithologies. Overall, clay content decreases downcore, and the coarsest samples occur at the bottom of the cored interval at Site C0021 (Fig. **F8**). No obvious particle size differences occur between MTD and non-MTD samples (Figs. **F7, F8**). However, samples from MTD-A plot within both the silty clay and clayey silt fields, whereas samples from MTD-B are exclusively in the clayey silt field.

Acknowledgments

The Integrated Ocean Drilling Program (IODP) provided samples for this research. Funding was provided by the Consortium for Ocean Leadership. We thank the IODP Expedition 338 science party and crew aboard the R/V *Chikyu* and at the Kochi Coring Facility for processing and shipping samples. We thank Julia Reece for a thorough and helpful review.

References

ASTM International, 2003. Standard test method for particle-size analysis of soils (Standard D422-63[2002]). In *Annual Book of ASTM Standards* (Vol. 04.08): *Soil and Rock* (I): West Conshohocken, PA (Am. Soc. Testing Mater.), 10–17. **http://www.astm.org/DATABASE.CART/HISTORICAL/D422-63R02.htm**

Germaine, J.T., and Germaine, A.V., 2009. *Geotechnical Laboratory Measurements for Engineers:* Hoboken, NJ (Wiley). **doi:10.1002/9780470548790**

Sawyer, D.E., Flemings, P.B., Buttles, J., and Mohrig, D., 2012. Mudflow transport behavior and deposit morphology: role of shear stress to yield strength ratio in subaqueous experiments. *Mar. Geol.*, 307–310:28-39. **doi:10.1016/j.margeo.2012.01.009**

Sawyer, D.E., Jacoby, R., Flemings, P., and Germaine, J.T., 2008. Data report: particle size analysis of sediments in the Ursa Basin, IODP Expedition 308 Sites U1324 and U1322, northern Gulf of Mexico. *In* Flemings, P.B., Behrmann, J.H., John, C.M., and the Expedition 308 Scientists, *Proc. IODP,* 308: College Station, TX (Integrated Ocean Drilling Program Management International, Inc.). **doi:10.2204/iodp.proc.308.205.2008**

Shepard, F.P., 1954. Nomenclature based on sand-silt-clay ratios. *J. Sediment. Res.,* 24(3):151–158. **doi:10.1306/D4269774-2B26-11D7-8648000102C1865D**

Strasser, M., Dugan, B., Kanagawa, K., Moore, G.F., Toczko, S., Maeda, L., Kido, Y., Moe, K.T., Sanada, Y., Esteban, L., Fabbri, O., Geersen, J., Hammerschmidt, S., Hayashi, H., Heirman, K., Hüpers, A., Jurado Rodriguez, M.J., Kameo, K., Kanamatsu, T., Kitajima, H., Masuda, H., Milliken, K., Mishra, R., Motoyama, I., Olcott, K., Oohashi, K., Pickering, K.T., Ramirez, S.G., Rashid, H., Sawyer, D., Schleicher, A., Shan, Y., Skarbek, R., Song, I., Takeshita, T., Toki, T., Tudge, J., Webb, S., Wilson, D.J., Wu, H.-Y., and Yamaguchi, A., 2014. Expedition 338 summary. *In* Strasser, M., Dugan, B., Kanagawa, K., Moore, G.F., Toczko, S., Maeda, L., and the Expedition 338 Scientists, *Proc. IODP,* 338: Yokohama (Integrated Ocean Drilling Program). **doi:10.2204/iodp.proc.338.101.2014**

Strasser, M., Moore, G.F., Kimura, G., Kopf, A.J., Underwood, M.B., Guo, J., and Screaton, E.J., 2011. Slumping and mass transport deposition in the Nankai forearc: evidence from IODP drilling and 3-D reflection seismic data. *Geochem., Geophys., Geosyst.,* 12(5):Q0AD13. **doi:10.1029/2010GC003431**

Initial receipt: 23 January 2014
Acceptance: 1 October 2014
Publication: 12 December 2014
MS 338-201

Figure F1. Sites C0021 and C0018 located ~100 km off Kii peninsula. Stars = locations of the 1944 and 1946 earthquakes. Red line = location of the subduction trench. Black line = seismic line (Fig. F2). (Modified from Strasser et al., 2014.)

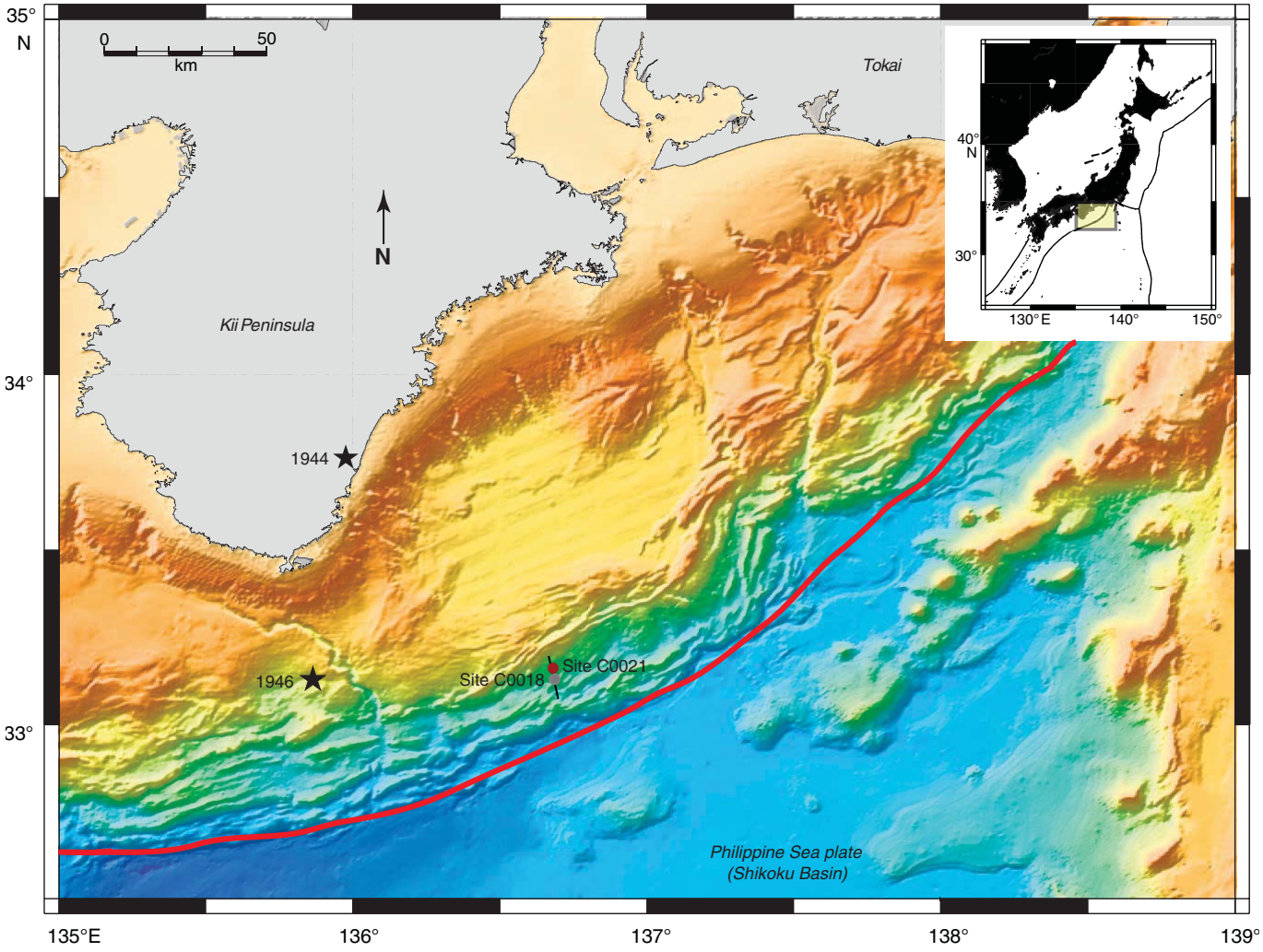

Figure F2. Seismic line A-A′ through Sites C0021 and C0018. Site C0021 line indicates total logging depth (294 mbsf). Coring only occurred between 83.6 and 194.5 mbsf. VE = vertical exaggeration. (From Strasser et al., 2014.)

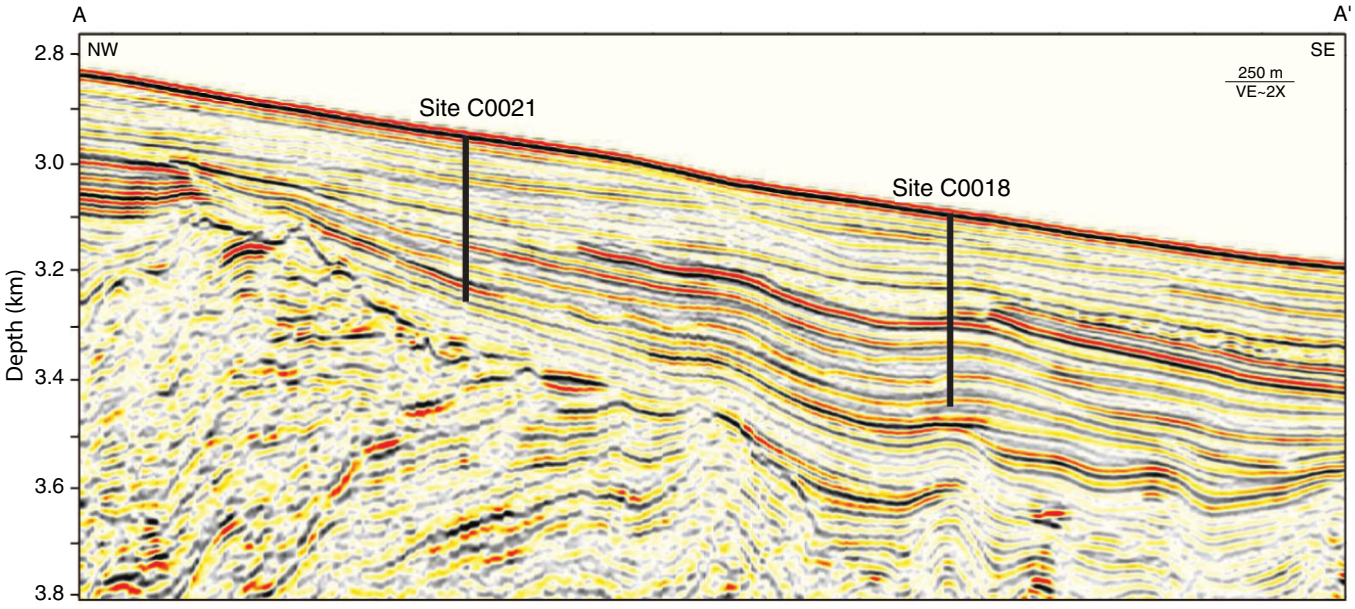

Figure F3. Shepard (1954) classification ternary diagram based on relative percentages of sand, silt, and clay.

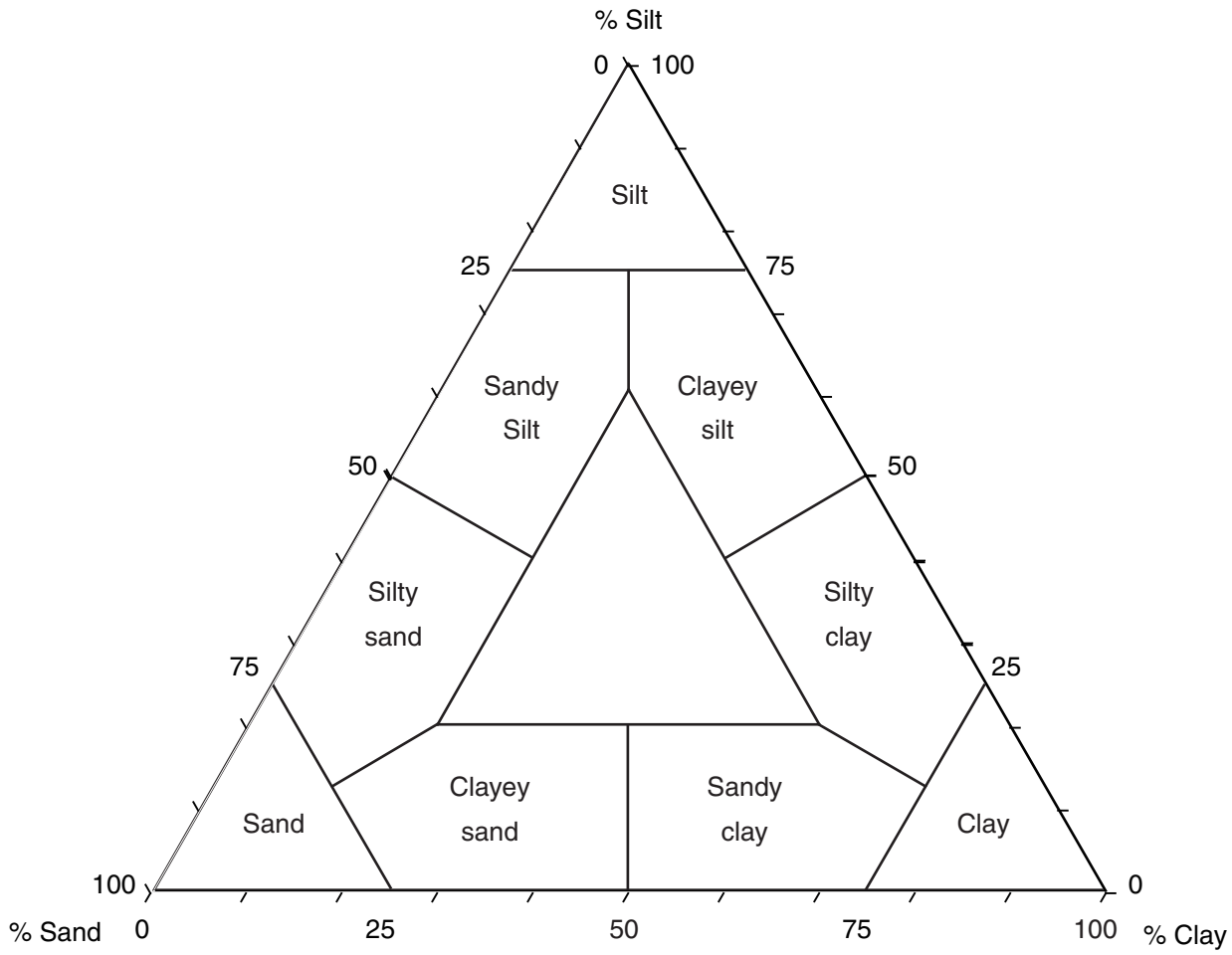

Figure F4. Sample data sheet for hydrometer analysis. Hr = hydrometer reading, effective depth = depth (L in Eq. 1) of hydrometer's center corrected for viscosity. Data sheets for all experiments are available in HYDROMETER in **"Supplementary material."**

Hydrometer Analysis

Project: Kumano 338-C0021
Test Number: 9H-8
Tested by: ZTM
Test Date: 12/2/2013

Boring: C0021
Sample: 9H-8
Location: 155.54mbsf

Hydrometer
Type: 151H Fisher Brand
Number: 98
Volume = 72 cm^3
Hr @ 1035 = 5.912 cm
Hr @ 1000 = 15.212 cm
Meniscus = 0.8 g/L

•Dispersing agent: Sodium Hexametaphosphate
•Dispersing agent not included in sample dry mass

Assumed Specific Gravity: 2.70
Measured Dry Sample Mass: 25.54 g
Measured Dispersing Aggent Mass: 6.25 g
Mass Lost From Readings: 2.00 g

Measurements				Constants		Results	
Elapsed Time (min.)	Susp'n Reading (g/L)	Water + Disp'nt Reading (g/L)	Temp. (°C)	Viscosity ($g\text{-}s/cm^2$)	Effective Depth (cm)	% Finer (%)	Diameter (mm)
0.25	1020.1	1004.0	23.1	9.54375E-06	9.631032735	100.12	0.080549
0.5	1019.9	1004.0	23.1	9.54375E-06	9.684390257	98.88	0.057115
1	1019.5	1004.0	23.1	9.54375E-06	9.791105301	96.39	0.040608
2	1019.2	1004.0	23.1	9.54375E-06	9.871141584	94.52	0.028831
4	1018.8	1004.0	23.1	9.54375E-06	9.977856628	92.04	0.020497
8	1018.0	1004.0	23.1	9.54375E-06	10.19128672	87.06	0.014648
16	1017.0	1004.0	23.1	9.54375E-06	10.45807433	80.84	0.010492
32	1016.0	1004.0	23.1	9.54375E-06	10.72486194	74.62	0.007513
64	1015.0	1004.0	23.1	9.54375E-06	10.99164955	68.40	0.005378
128	1013.5	1004.0	23.1	9.54375E-06	11.39183096	59.08	0.003872
256	1012.0	1004.0	23.1	9.54375E-06	11.79201238	49.75	0.002785
517	1011.0	1004.0	23.1	9.54375E-06	12.05879999	43.53	0.001982
697	1010.5	1004.0	23.1	9.54375E-06	12.19219379	40.42	0.001716
2897	1009.1	1004.0	23.1	9.54375E-06	12.56569645	31.71	0.000855

Sieve Data (wet sieved at 62.5µm)
Mass retained on sieve (grams): 0.600
Sand-% of dry mass: 2.30
% passing 0.0625 mm: 97.70

0.0625

Interpolated value at silt/sand boundary (2µm)

% Finer	Diameter (mm)
44.60	0.002

Remarks/Comments: drying pan 3 (490.19g); dry mass plus pan (519.98)
dry mass= 29.79 g

Final Data

% Sand	% Silt	% Clay
2.30	54.13	43.58

Figure F5. Sample particle size distribution plot on a semilog scale (Sample 338-C0021B-9H-8, 69–71 cm; 155.53 mbsf). Black dots = hydrometer readings. Sand/silt boundary is defined at 62.5 µm; silt/clay boundary is defined at 2 µm.

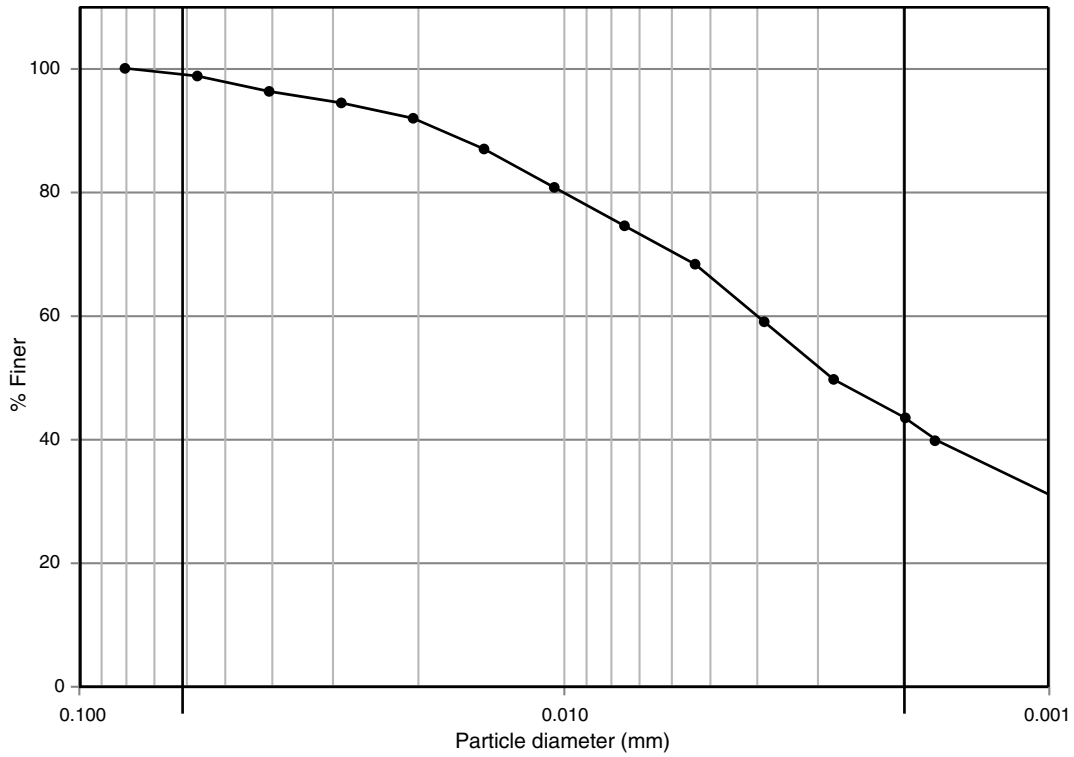

Figure F6. Hydrometer results for 49 samples, Hole C0021B. Thirty-eight samples (76%) plot as clayey silt, 16% (8) plot as silty clay, and 8% (4) plot in sandy clay, sandy silt, silt, and sand-silt-clay.

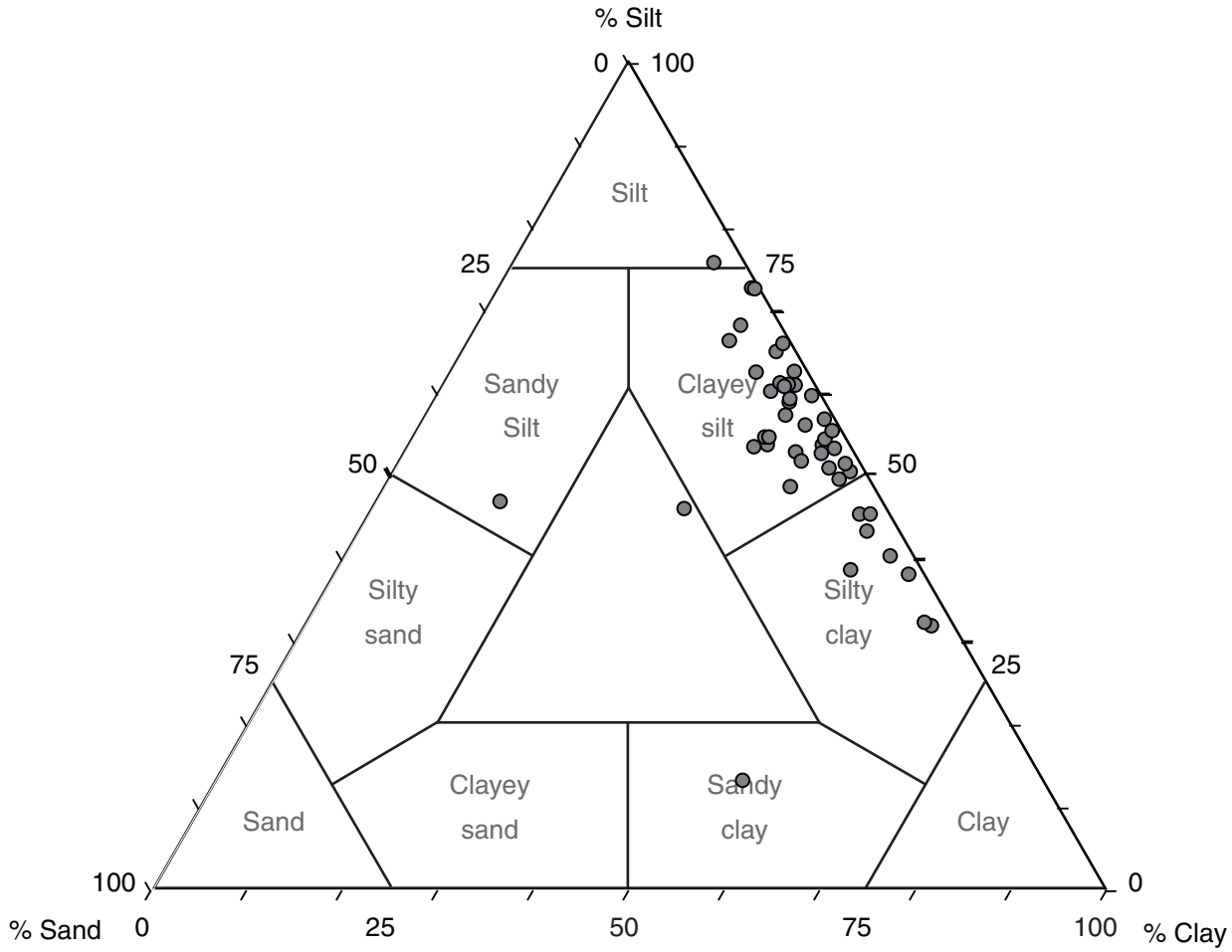

Figure F7. Hydrometer results color-coded by mass transport deposit (MTD), Hole C0021B.

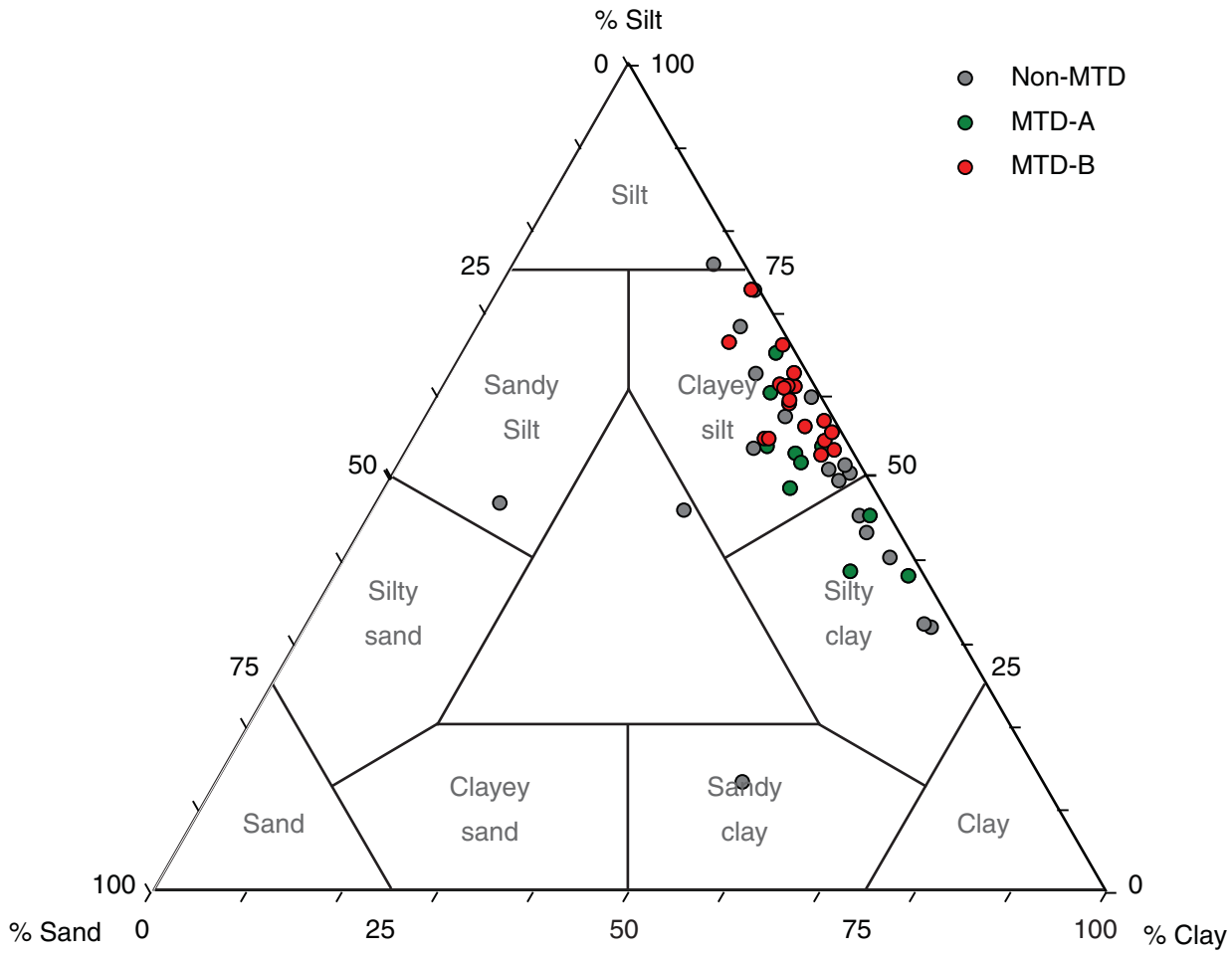

Figure F8. Plot of particle size distribution with LWD gamma ray and resistivity, Hole C0021B. Mass transport deposits (MTD) MTD-A and MTD-B occur at 94–117 and 135–176 mbsf (Strasser et al., 2011).

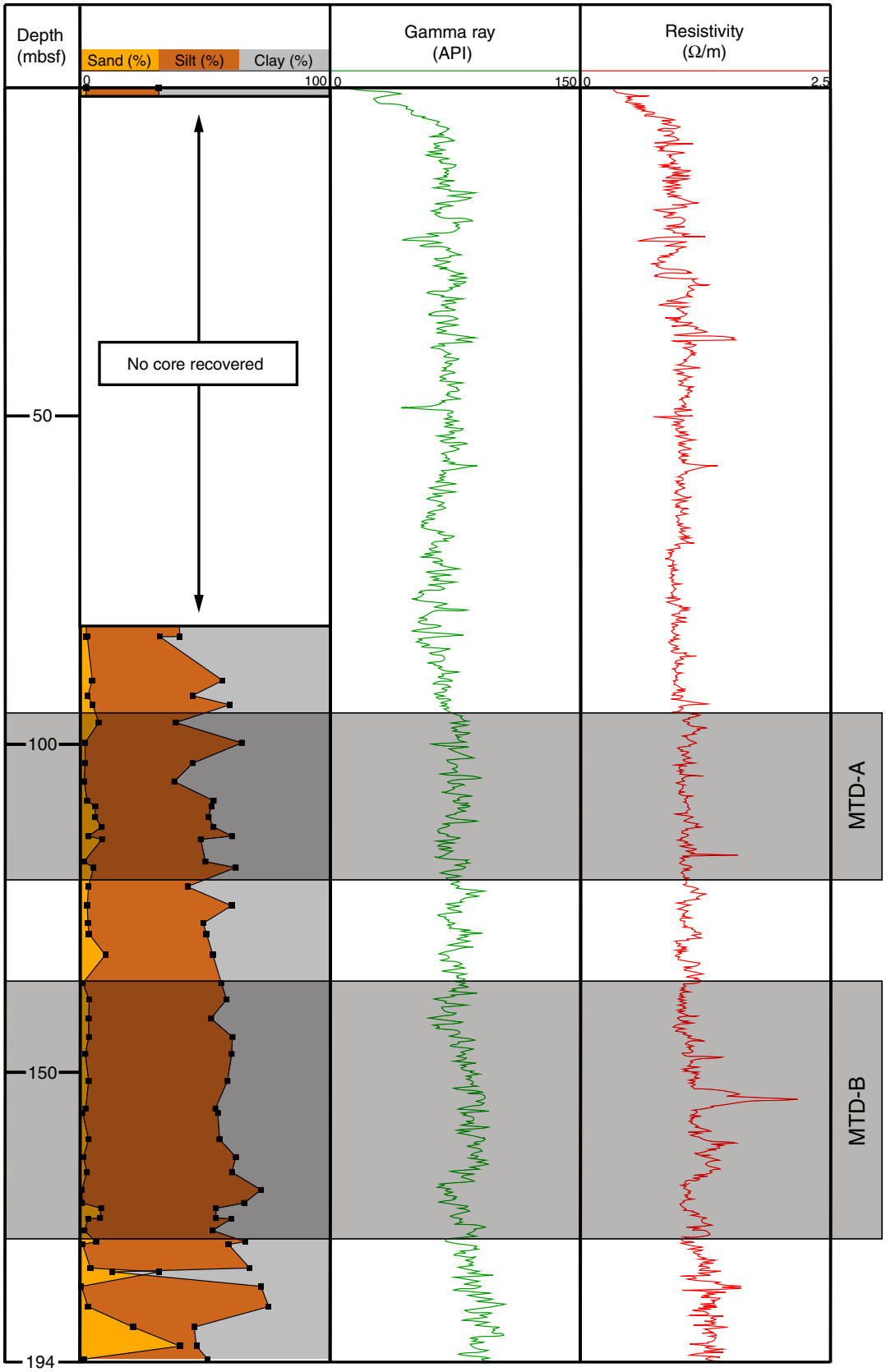

Table T1. Particle size analysis, Hole C0021B.

Core, section, interval (cm)	Depth (mbsf)	Particle size (%)			Mass transport deposit
		Sand	Silt	Clay	
338-C0021B-					
1H-1	0.06	2.45	31.51	66.04	
1H-5, 38–40	83.60	2.53	39.96	57.51	
1H-5, 40–42	83.62	2.97	31.92	65.11	
3H-2	90.30	4.95	57.03	38.02	
3H-5	92.60	3.19	45.02	51.79	
3H-6	94.00	5.04	59.92	35.04	MTD-A
3H-8	96.70	7.51	38.29	54.20	MTD-A
4H-1	99.80	2.08	64.72	33.20	MTD-A
4H-4	102.90	2.08	45.04	52.88	MTD-A
4H-6	105.70	1.72	37.74	60.54	MTD-A
4H-8	108.60	2.90	53.4	43.70	MTD-A
5H-1	109.50	6.11	52.58	41.31	MTD-A
5H-3	111.10	6.08	51.47	42.45	MTD-A
5H-4	112.60	8.66	53.43	37.91	MTD-A
5H-5	114.00	3.43	60.74	35.83	MTD-A
5H-6	114.50	8.80	48.34	42.86	MTD-A
5H-9	117.90	1.63	50.17	48.20	
6H-2	118.80	5.43	62.23	32.34	
6H-5	121.70	3.46	42.96	53.58	
6H-7	124.60	2.94	60.66	36.40	
6H-9	127.30	3.22	49.26	47.52	
7H-2	128.90	3.60	50.61	45.79	
7H-6	132.10	10.19	53.17	36.64	
7H-9	136.40	1.14	56.55	42.31	MTD-B
8H-3	138.90	3.75	58.63	37.62	MTD-B
8H-5	141.80	3.51	52.39	44.10	MTD-B
8H-7	144.60	3.58	60.94	35.48	MTD-B
9H-1	147.20	2.11	60.69	37.20	MTD-B
9H-5	151.30	3.50	59.02	37.48	MTD-B
9H-8	155.50	2.29	54.13	43.58	MTD-B
10H-2	156.20	1.03	55.13	43.84	MTD-B
10H-5	160.20	3.48	55.84	40.68	MTD-B
10H-9	162.90	1.38	62.33	36.29	MTD-B
11H-1	165.20	2.80	60.75	36.45	MTD-B
11H-3	167.90	0.81	72.41	26.78	MTD-B
11H-5	169.90	0.87	65.72	33.41	MTD-B
12H-3	170.70	8.46	54.37	37.17	MTD-B
12H-4, 59–61	172.20	8.00	54.37	37.63	MTD-B
12H-4, 74–76	172.30	3.32	60.52	36.16	MTD-B
12H-6	174.10	1.85	53.00	45.15	MTD-B
13T-1, 31–33	175.80	6.34	66.03	27.63	MTD-B
13T-1, 73–75	176.20	1.04	59.38	39.58	
13T-5	179.80	4.22	67.91	27.87	
13T-6	180.40	31.54	12.80	55.66	
13T-8	182.60	0.54	72.31	27.15	
14T-1	185.70	3.23	75.48	21.29	
14T-4	188.80	21.21	45.70	33.09	
14T-6	191.70	40.06	46.57	13.37	
14T-8	193.70	1.63	51.15	47.22	

Table T2. Nomenclature.

Variable	Meaning	Dimensions	Value
H	Distance particle falls	cm	Variable
ρ_w	Mass density of water	g/cm^3	0.9975412
G_s	Specific gravity	Dimensionless	2.70
μ	Viscosity of fluid	mPa·s	9.53×10^{-6}
t	Time for fall	Minutes	Variable
g	Acceleration due to gravity	cm/s^2	980
D	Diameter of particle	mm	Variable
N_m	Percent finer material at reading m	Percent	Variable
V	Volume of suspension	cm^3	1000
M_D	Dry soil mass of hydrometer specimen	g	Variable
ρ_c	Mass density of water at the calibration temperature	g/cm^3	0.9975412
r_m	Hydrometer reading in suspension at time, t, and temperature, T	Dimensionless	Variable
$r_{w,m}$	Hydrometer reading in water with dispersant at the same temperature as for r_m	Dimensionless	1004.0
m	Reading number		